

limit, $3 < a < 5$ for the Al, Fe and Cu targets. Almost invariably the theoretical cross sections increased with a as expected.

The second parameter varied was r_0 , which appears in the formula for the radius, $r = r_0 A^{1/3}$ F. Calculations were made for a nuclear radius parameter of 1.5 F and then 1.7 F. In general, the use of the latter value resulted in larger predicted cross sections and a shifting of peak positions to lower energies. The dashed curve of Fig. 4 shows the excitation function calculated from the compound nucleus theory using the parameter $r_0 = 1.5$ and $a = 3.0$. Fig. 8 makes a comparison between experi-

ment and the evaporation theory with four choices of the parameters.

ACKNOWLEDGMENTS

The authors wish to acknowledge the invaluable assistance of Miss Mavis George in processing much of the data and of Dr. R. L. Hahn who introduced us to the FORTRAN program for making nuclear-evaporation calculations. Also thanks are due to the operating staff of the Oak Ridge Isochronous Cyclotron for their cooperation.

Analysis of the $\text{Ca}^{40}(d,p)\text{Ca}^{41}$ Reaction

S. T. BUTLER, R. G. L. HEWITT, AND J. S. TRUELOVE

Department of Theoretical Physics, University of Sydney, Sydney, New South Wales, Australia

(Received 8 June 1967)

The method recently developed by Butler, Hewitt, McKellar, and May (BHMM) is used in an analysis of the $\text{Ca}^{40}(d,p)\text{Ca}^{41}$ ground-state reaction for six different deuteron energies. The BHMM expression for the (d,p) differential cross section depends only on neutron and proton elastic-scattering wave functions. In the present work, these are generated by optical parameters so chosen as to give elastic-scattering cross sections in satisfactory agreement with experiment. The (d,p) angular distributions are then also found to be in good agreement with experiment. It is determined that the spectroscopic factor relating to the $\text{Ca}^{40}\text{-Ca}^{41}$ overlap has the value 0.56 ± 0.04 .

1. INTRODUCTION

THE method recently developed by Butler, Hewitt, McKellar, and May¹ (hereafter referred to as BHMM) is used in an analysis of the $\text{Ca}^{40}(d,p)\text{Ca}^{41}$ ground-state reaction for six different deuteron energies.

The BHMM expression for the (d,p) differential cross section depends only on neutron and proton elastic-scattering wave functions. In the present work, these are generated by optical parameters so chosen as to give elastic-scattering cross sections in satisfactory agreement with experiment for both neutrons and protons at appropriate energies.

The averaged parameter set of Perey and Buck² for neutron scattering and that of Buck³ for proton scattering are chosen as a starting point. It is found that these parameters will generate elastic-scattering cross sections in consistent agreement with experiment for scattering on Ca^{40} with two simple modifications:

(a) The surface diffuseness parameters (a, b) must be reduced to $(a\lambda, b\lambda)$ with $\lambda = 0.80$, for both neutron and proton sets. This presumably reflects the fact that the Ca^{40} nucleus has a somewhat sharper surface than average nuclei.

(b) The strengths W_N, W_P of the imaginary optical

potentials for neutron and proton scattering must in general be altered from the averaged values. For neutrons, we find $W_N = 5.4$ MeV is required for 6-MeV scattering and $W_N = 7.0$ MeV for 14-MeV scattering. For protons, we find $W_P = 6.0$ MeV for 14.6-MeV scattering and $W_P = 7.0$ MeV for 17.3-MeV scattering. In each case we assume a linear interpolation between the two energies.

The BHMM differential cross sections for the $\text{Ca}^{40}(d,p)\text{Ca}^{41}$ reaction are then calculated without further adjustment of these parameters and compared with experiment⁴ at six deuteron energies from 7 to 12 MeV. Agreement is good at all energies. Typical of this agreement are the 12-MeV results shown, together with experimental points, in Fig. 1. The neutron orbital angular momentum is, of course, given by $l = 3$ and the BHMM results of Fig. 1 require a spectroscopic factor $S = 0.60$. (It is to be noted that the less accurate value obtained in Ref. 1 using simple averaged optical parameters, without heed to elastic scattering, was $S \approx 0.5$).

For comparison purposes we also show the results of corresponding distorted-wave Born analysis (DWBA) made by Lee, Schiffer, Zeidman, Satchler, Drisko, and Bassel⁴ at each energy, the comparison at 12 MeV being shown in Fig. 1. It is found that the BHMM and DWBA angular distributions are in comparable agreement with

¹ S. T. Butler, R. G. L. Hewitt, B. H. J. McKellar, and R. M. May, *Ann. Phys. (N. Y.)* **23**, 282 (1967).

² F. Perey and B. Buck, *Nucl. Phys.* **32**, 353 (1962).

³ B. Buck, *Phys. Rev.* **130**, 712 (1963).

⁴ L. L. Lee, J. P. Schiffer, B. Zeidman, G. R. Satchler, R. M. Drisko, and R. H. Bassel, *Phys. Rev.* **136**, B971 (1964).

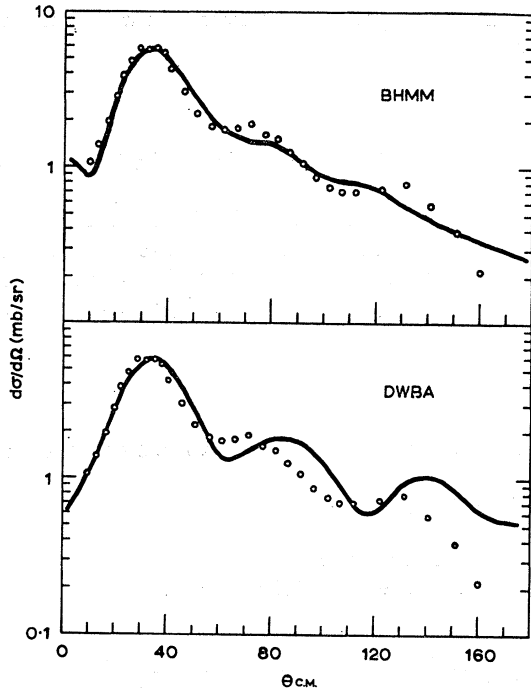


FIG. 1. Comparison of the predictions of BHMM and DWBA for the $\text{Ca}^{40}(d,p)\text{Ca}^{41}$ ground-state reaction at 12 MeV. The DWBA curve was generated with a "best fit" type-Z deuteron potential (Ref. 4). The experimental points are also obtained from Ref. 4.

experiment from an over-all point of view. On the other hand, the BHMM spectroscopic factors are significantly smaller than those obtained by DWBA analysis, while being equally as stable against variations in incident deuteron energy. Specifically, the spectroscopic factors obtained in this paper for the six integral deuteron energies from 7 to 12 MeV are 0.49, 0.52, 0.55, 0.57, 0.60, and 0.60, respectively. The corresponding values⁴ from DWBA analysis with "best Z" parameters are 0.74, 0.93, 0.89, 0.83, 0.96, and 0.83, respectively.

In Sec. 2 of this paper we briefly present the development of BHMM and discuss some points not referred to in Ref. 1. Section 3 defines the parameter sets used to generate the elastic-scattering nucleon wave functions and shows comparisons with experiment for nucleon elastic scattering and the $\text{Ca}^{40}(d,p)\text{Ca}^{41}$ cross sections. In Sec. 4, we discuss the results and, in particular, why the value of $S=0.56\pm 0.04$ for the spectroscopic factor can be considered reasonable despite the higher value obtained from DWBA analysis.

2. FORMAL THEORY

The exact many-body matrix element for the full (d,p) process, which we denote by \mathfrak{M} , may be written as⁵

$$\mathfrak{M}(\kappa, \mathbf{k}_p) = \langle \Psi^-(\kappa, \mathbf{k}_p) | V_{np} | \Psi_d^+ \rangle, \quad (1)$$

⁵ M. L. Goldberger and K. M. Watson, *Collision Theory* (John Wiley & Sons, Inc., New York, 1964).

where $\Psi^-(\kappa, \mathbf{k}_p)$ is the complete many-body wave function representing a proton with momentum $\hbar\mathbf{k}_p$ [equal to that of the final proton momentum in the (d,p) reaction] incident on the initial or core nucleus; the incoming spherical-wave solution is to be chosen. The argument κ relates to the neutron being in a specified bound state with binding energy, relative to the core state, of $\hbar^2\kappa^2/2m$. Thus Ψ^- satisfies the wave equation

$$(H_x + T_n + T_p + V_{nx} + V_{px} - E_T)\Psi^- = 0, \quad (2)$$

where E_T is the total energy of the system, H_x is the Hamiltonian of the initial core nucleus X , T_n , and T_p are kinetic-energy operators, and V_{nx} and V_{px} are the neutron and proton interactions with X , respectively.

Similarly, Ψ_d^+ represents the complete wave function, with outgoing spherical waves, for a deuteron of momentum $\hbar\mathbf{k}_d$ incident on the initial nucleus. Thus Ψ_d^+ satisfies the wave equation

$$(H + T_n + T_p + V_{nx} + V_{px} - E_T)\Psi_d^+ = -V_{np}\Psi_d^+. \quad (3)$$

The conventional continuum normalization⁵ is used for all many-body wave functions.

The direct reaction matrix element, which is expected to dominate the process, is obtained from \mathfrak{M} by a projection on the core state. Denoting this by \mathfrak{M}_C we have

$$\mathfrak{M}_C = \langle \Lambda_C \Psi^- | V_{np} | \Psi_d^+ \rangle \quad (4a)$$

$$= \langle \Lambda_C \Psi^- | V_{np} | \Lambda_C \Psi_d^+ \rangle \quad (4b)$$

$$= \langle \Psi^- | V_{np} | \Lambda_C \Psi_d^+ \rangle, \quad (4c)$$

where Λ_C is the core-state projection operator. The assumption that the direct process is dominant implies that one can or cannot include a Λ_C as one pleases, with the expectation of little change in the matrix element.

The method developed in BHMM is based on a transformation of Eq. (4) to an alternative form. An expansion of \mathfrak{M}_C is performed in terms of the complete set of wave functions $\Psi^+(\mathbf{k}_n', \mathbf{k}_p')$ generated by Eq. (2), with $E_T = E_C + E_n' + E_p'$, where E_C is the core energy. For continuum energies, the asymptotic form of Ψ^+ represents plane wave neutrons and protons with momenta $\hbar\mathbf{k}_n'$ and $\hbar\mathbf{k}_p'$ incident on the core nucleus, with outgoing scattered waves; the full set Ψ^+ must also include discrete neutron and proton states designated by κ_n' and κ_p' , respectively.

Thus it is straightforward to expand \mathfrak{M}_C as

$$\mathfrak{M}_C = \int_{\Sigma} d\mathbf{k}_p' \int_{\Sigma} d\mathbf{k}_n' \langle \Lambda_C \Psi^-(\kappa, \mathbf{k}_p) | \Psi^+(\mathbf{k}_n', \mathbf{k}_p') \rangle \times \langle \Psi^+(\mathbf{k}_n', \mathbf{k}_p') | V_{np} | \Lambda_C \Psi_d^+ \rangle, \quad (5)$$

where the Σ notation implies summation as well as integration. The interesting point here is that the specific term $\mathbf{k}_n' = \kappa$ can immediately be identified. As shown in BHMM it is simply $S\mathfrak{M}_C$, where S is the spectroscopic factor for the reaction.

A matrix element \mathfrak{M}_S may thus be defined which omits this term

$$\mathfrak{M}_S = \int_{\Sigma} d\mathbf{k}_p' \int_{\Sigma \neq \kappa} d\mathbf{k}_n' \langle \Lambda_C \Psi^-(\kappa, \mathbf{k}_p) | \Psi^+(\mathbf{k}_n', \mathbf{k}_p') \rangle \times \langle \Psi^+(\mathbf{k}_n', \mathbf{k}_p') | V_{np} | \Lambda_C \Psi_d^+ \rangle, \quad (6)$$

so that

$$\mathfrak{M}_S = (1 - S)\mathfrak{M}_C. \quad (7)$$

Now \mathfrak{M}_S is more amenable to manipulation than the full \mathfrak{M}_C . For rigor let us consider the set Ψ^+ to have originally been defined with a small imaginary contribution $i\eta$ to the energy; thus η is the conventional convergence factor.⁵ As remarked before, the assumption that the direct process is dominant implies that we may remove the Λ_C operator from the right-hand side of the V_{np} matrix element in Eq. (6), without significantly altering the result (see Appendix). Then the left-hand side of Eq. (3) may be used for $V_{np}\Psi_d^+$ in Eq. (6). Moreover, the Hamiltonian operators may be operated to the left, and we find

$$\langle \Psi^+(\mathbf{k}_n', \mathbf{k}_p') | V_{np} | \Psi_d^+ \rangle = \lim_{\eta \rightarrow 0} -(E_n' + E_p' - E_n - E_p - i\eta) \times \langle \Psi^+(\mathbf{k}_n', \mathbf{k}_p') | \Psi_d^+ \rangle, \quad (8)$$

where E_n' and E_p' are the energies associated with \mathbf{k}_n' and \mathbf{k}_p' , respectively, E_n is the energy of the neutron in its final state κ —that is, $\hbar^2\kappa^2/2m$ —and E_p is the final proton energy $\hbar^2k_p^2/2m$. It is, however, subsequently found that $E_p' = E_p$, and in anticipation of this we may write

$$\langle \Psi^+(\mathbf{k}_n', \mathbf{k}_p') | V_{np} | \Psi_d^+ \rangle = \lim_{\eta \rightarrow 0} -(E_n' - E_n - i\eta) \times \langle \Psi^+(\mathbf{k}_n', \mathbf{k}_p') | \Psi_d^+ \rangle. \quad (9)$$

The full significance of why the term $\mathbf{k}_n' = \kappa$ is excluded in the definition of \mathfrak{M}_S [Eq. (6)] can now be appreciated. For this term, and this term only, $E_n' = E_n$. The energy difference $(E_n' - E_n - i\eta)$ tends to zero in the limit $\eta \rightarrow 0$, and the actual value of Eq. (9) in this instance depends in detail on the precise form of the energy singularity in $\langle \Psi^+(\kappa, \mathbf{k}_p) | \Psi_d^+ \rangle$. Any of the usual approximations to Ψ_d^+ would lose this singularity, and Eq. (9) would erroneously appear to be zero. Having isolated the term $\mathbf{k}_n' = \kappa$ from Eq. (5), and identifying it as $S\mathfrak{M}_C$, no such difficulty arises in Eq. (6), where $\mathbf{k}_n' \neq \kappa$. Here $E_n' \neq E_n$, and Eq. (9) may be used for the integrand factor $\langle \Psi^+(\mathbf{k}_n', \mathbf{k}_p') | V_{np} | \Psi_d^+ \rangle$ without difficulty; the limiting process with respect to η is trivial.

A motivation of BHMM for using \mathfrak{M}_S for the evaluation of the direct-reaction cross section is to explore the use of the impulse approximation for Ψ_d^+ which is written in the form

$$\Psi_d^+ = \frac{(4\pi)^{1/2}N}{(2\pi)^{3/2}} \int d\mathbf{k}_p' G(\mathbf{k}_d, \mathbf{k}_p') \Psi^+(\mathbf{Q}', \mathbf{k}_p'), \quad (10)$$

where Ψ^+ is an eigenfunction of the Hamiltonian of Eq. (3) corresponding to a neutron momentum $\mathbf{k}_n' = \mathbf{Q}' = \mathbf{k}_d - (A/A+1)\mathbf{k}_p'$ with A the mass number of the initial nucleus. The constant N arises from the normalization of the free-deuteron internal wave function $\chi(r)$ which is taken to have the Hulthén form

$$\chi(r) = (4\pi)^{-1/2}N \{e^{-\gamma r} - e^{-\zeta r}\}/r, \quad (11)$$

so that N normalizes the radial part of χ to unity. The function G then has the form

$$G(\mathbf{k}_d, \mathbf{k}_p) = \left\{ \frac{1}{(\mathbf{k}_d/2 - \mathbf{k}_p)^2 + \gamma^2} - \frac{1}{(\mathbf{k}_d/2 - \mathbf{k}_p)^2 + \zeta^2} \right\}. \quad (12)$$

Substitution of the impulse approximation of Eq. (10) directly into \mathfrak{M}_C [Eq. (4)] yields an expression which appears highly intractable. The evaluation can immediately proceed, however, via \mathfrak{M}_S , for the substitution of Eq. (10) into Eq. (9) yields the result

$$\langle \Psi^+(\mathbf{k}_n', \mathbf{k}_p') | V_{np} | \Psi_d^+ \rangle = -\frac{(4\pi)^{1/2}\hbar^2N}{(2\pi)^{3/2}m} g(\mathbf{k}_d, \mathbf{k}_p') \delta(\mathbf{k}_n' - \mathbf{Q}), \quad (13)$$

with

$$g(\mathbf{k}_d, \mathbf{k}_p') = 1 - \frac{(\mathbf{k}_d/2 - \mathbf{k}_p')^2 + \gamma^2}{(\mathbf{k}_d/2 - \mathbf{k}_p')^2 + \zeta^2}. \quad (14)$$

If we denote the value of \mathfrak{M}_S under the impulse approximation by $\mathfrak{M}_S(I)$, we have

$$\mathfrak{M}_S(I) = -\frac{(4\pi)^{1/2}\hbar^2N}{(2\pi)^{3/2}m} \int d\mathbf{k}_p' g(\mathbf{k}_d, \mathbf{k}_p') \times \langle \Lambda_C \Psi^-(\kappa, \mathbf{k}_p) | \Psi^+(\mathbf{Q}', \mathbf{k}_p') \rangle. \quad (15)$$

This is related to the full direct reaction matrix element under impulse approximation $\mathfrak{M}_C(I)$ by

$$\mathfrak{M}_S(I) = (1 - S)\mathfrak{M}_C(I). \quad (16)$$

An evaluation of $\mathfrak{M}_S(I)$ [Eq. (15)] is thus equivalent to a full evaluation of $\mathfrak{M}_C(I)$.

The evaluation of \mathfrak{M}_S from Eq. (15) is performed in the manner described in BHMM. After integration over core coordinates, we have

$$\mathfrak{M}_S = S^{1/2}M_S, \quad (17)$$

where

$$M_S = -\frac{(4\pi)^{1/2}\hbar^2N}{(2\pi)^{3/2}m} \int d\mathbf{k}_p' g(\mathbf{k}_d, \mathbf{k}_p') \langle F i^m(\mathbf{r}_n) | \psi_n^+(\mathbf{Q}', \mathbf{r}_n) \rangle \times \langle \psi_p^-(\mathbf{k}_p, \mathbf{r}_p) | \psi_p^+(\mathbf{k}_p', \mathbf{r}_p) \rangle, \quad (18)$$

The wave functions ψ_n and ψ_p are optical wave functions for elastic scattering of the neutron and proton, respectively, by the core nucleus, and F is the normalized single-particle wave function of the captured neutron.

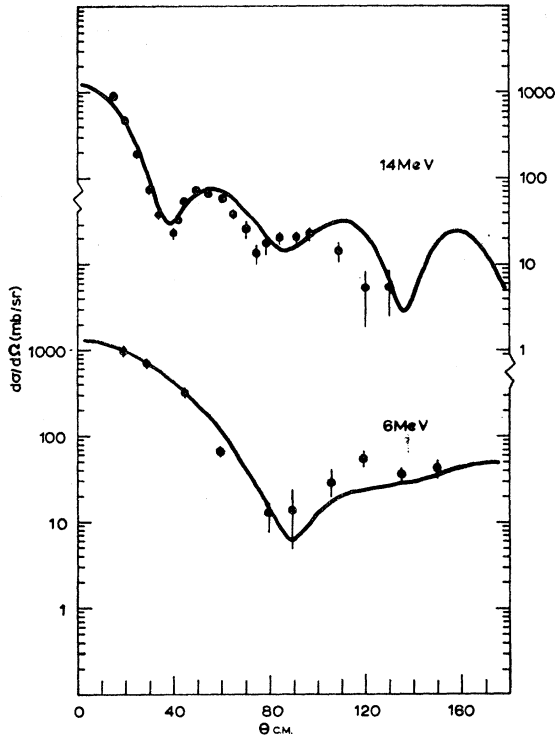


FIG. 2. Theoretical and experimental neutron elastic-scattering cross sections at 6 and 14 MeV. The theoretical curves were generated with the parameters detailed in Sec. 3. The experimental points were obtained from Refs. 7 and 6, respectively.

The total direct-reaction cross section is then

$$\frac{d\sigma}{d\Omega}(S \neq 1) = \frac{\frac{1}{2}m_p m_d k_p (2J_f + 1)}{(2\pi\hbar^2)^2 k_d (2J_i + 1)} \times \frac{1}{(2l+1)} \frac{1}{(1-S)^2} (2\pi)^6 \sum_m |M_S|^2. \quad (19)$$

The extension to include spin-dependent effects is straightforward and is outlined in Ref. 1.

Finally it should be noted that use of \mathfrak{N}_S —Eq. (6)—together with Eq. (9) has advantages quite apart from use of the sudden approximation. Contributions to Eq. (9), and thus to Eq. (6), arise overwhelmingly from

TABLE I. Nucleon optical parameters. Except for the imaginary potential strengths W_N , W_P and the surface diffuseness variation λ , they are the parameters of Perey and Buck for the neutron and of Buck for the proton.

Parameter	Neutron	Proton
V (MeV)	$48.0-0.29E$	$52.6-0.28E$
W (MeV)	W_N	W_P
R (F)	$1.27A^{1/3}$	$1.25A^{1/3}$
a (F)	0.66λ	0.65λ
b (F)	1.17λ	1.17λ
V_S (MeV)	7.2	8.0

asymptotic regions of configuration space where deuteron polarization is unimportant. Thus evaluation of Eq. (6) via Eq. (9) eliminates the difficulty associated with usual DWBA analysis based on Eq. (4) directly.

3. RESULTS

The method of calculation and the nucleon optical potential shapes are precisely as described in BHMM. The parameters of the optical potentials used are displayed in Table I. Except for the imaginary potential strengths W_N , W_P and the surface diffuseness parameter λ , they are the parameters of Perey and Buck² for the neutron and of Buck³ for the proton.

We have limited any adjustments to the three parameters W_N , W_P , and λ to restrict parameter variations within reasonable bounds. To start with, it is to be expected that Ca^{40} has a somewhat sharper surface than average nuclei, and it is known that the nucleon absorption parameters vary over the ranges of energies which enter in the evaluation of our results. It is reasonable, therefore, that these should provide the main adjustment of parameters required to give satisfactory agreement with elastic-scattering results.

Initially, therefore, we set out to achieve agreement, as closely as possible, with relevant elastic-scattering data. Neutron-scattering data on Ca^{40} are available

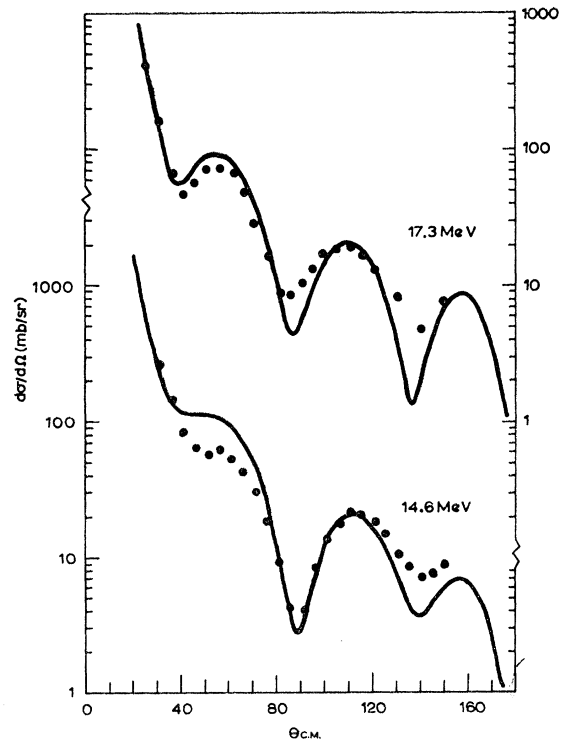


FIG. 3. Theoretical and experimental proton elastic-scattering cross sections at 14.6 and 17.3 MeV. The theoretical curves were generated with the parameters detailed in Sec. 3. The experimental points were obtained from Ref. 8.

TABLE II. Spectroscopic factors.

Quantity	Deuteron energy						Average
	7 MeV	8 MeV	9 MeV	10 MeV	11 MeV	12 MeV	
Peak magnitude (mb/sr)	4.2	4.4	5.15	5.37	6.55	5.65	
S (BHMM)	0.49	0.52	0.55	0.57	0.60	0.60	0.56 ± 0.04
S (DWBA) ^a	0.74	0.93	0.89	0.83	0.96	0.83	0.87 ± 0.07

^a Obtained with best Z parameters—zero-range approximation without deuteron spin-orbit coupling.

for 14 and 6 MeV.^{6,7} Since the most important range of neutron energies [i.e., those at which the wave functions $\psi_n^+(\mathbf{Q}, \mathbf{r}_n)$ are calculated] is from 4 to 14 MeV, these experimental results are sufficient for our present purpose. We have made various check runs which show that the results are essentially independent of the neutron imaginary potential for energies greater than 14 MeV. Similarly, the proton-scattering data which we use for fitting apply to 14.6- and 17.3-MeV protons.⁸ A

proton optical potential which reasonably generates elastic scattering at these two energies should also be suitable for our present purposes.

We find that, within the framework which we have permitted ourselves, best possible agreement with the above four sets of data is obtained with $\lambda=0.80$. The strength W_N of the neutron absorption potential is then found to be 5.4 MeV for scattering at 6 MeV and 7.0 MeV for scattering at 14 MeV. Therefore, for neutron energies E_n less than 14 MeV we assume a linear variation of W_N of the form

$$W_N = 4.2 + 0.2E_n, \quad E_n \leq 14. \quad (20)$$

The value of W_N for energies greater than 14 MeV is

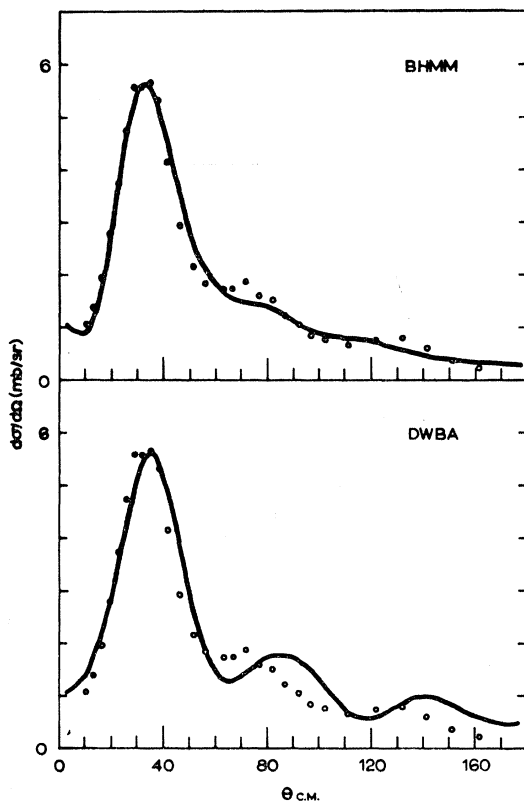


FIG. 4. Comparison of the predictions of BHMM and DWBA for the Ca⁴⁰(d, p)Ca⁴¹ ground-state reaction at 12 MeV. The DWBA curve was generated with a "best-fit" type- Z deuteron potential (Ref. 4). The experimental points are also obtained from Ref. 4.

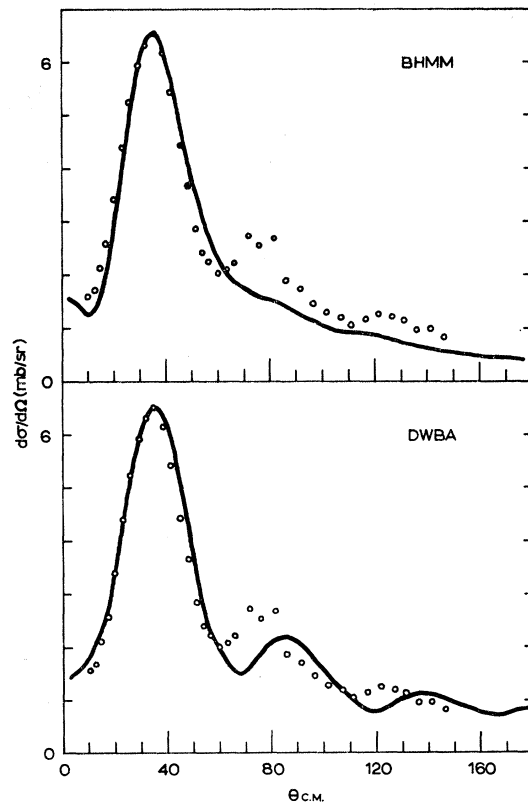


FIG. 5. Comparison of the predictions of BHMM and DWBA for the Ca⁴⁰(d, p)Ca⁴¹ ground-state reaction at 11 MeV. The DWBA curve was generated with a "best-fit" type- Z deuteron potential (Ref. 4). The experimental points are also obtained from Ref. 4.

⁶ *Proceedings of the Conference on Direct Interactions and Nuclear Reaction Mechanisms*, edited by E. Clementel and C. Villi (Gordon and Breach Science Publishers, Inc., New York, 1963), p. 103.

⁷ L. Rosen (private communication).

⁸ W. S. Gray, R. A. Kenefick, and J. J. Kraushaar, Nucl. Phys. 67, 542 (1965).

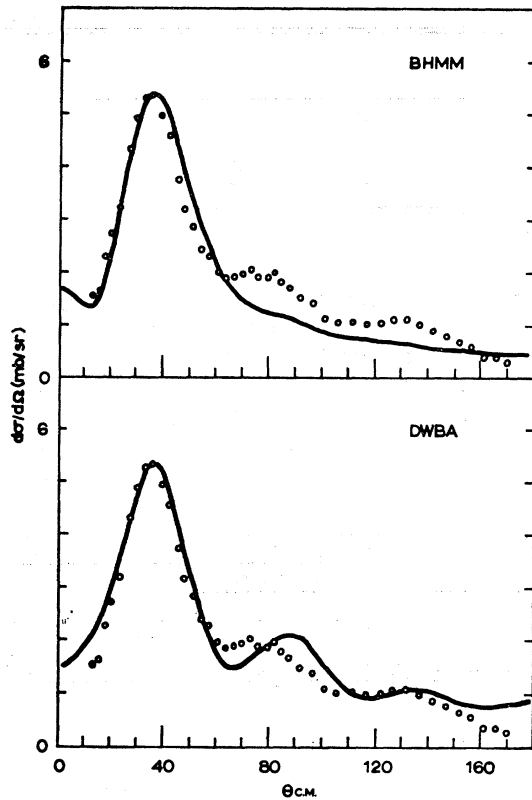


FIG. 6. Comparison of the predictions of BHMM and DWBA for the $\text{Ca}^{40}(d,p)\text{Ca}^{41}$ ground-state reaction at 10 MeV. The DWBA curve was generated with a "best-fit" type-Z deuteron potential (Ref. 4). The experimental points are also obtained from Ref. 4.

comparatively unimportant; we extend Eq. (20) with

$$W_N = 7.0 + 2.3 \ln(E_n/14), \quad E_n > 14. \quad (21)$$

The strength W_P of the proton absorption potential is found to be 6.0 MeV for 14.6-MeV scattering and 7.0 MeV for 17.3-MeV scattering; we assume a linear interpolation between these energies. Comparisons of the elastic scattering generated by these "best-fit" nucleon parameters with the four sets of scattering data are shown in Figs. 2 and 3.

The method of evaluation of the neutron bound-state function $F_l^m(\mathbf{r}_N)$ is as described in BHMM, the real potential depth being adjusted to yield the observed binding; for consistency the diffuseness parameter λ is taken to be the same as for the neutron scattering.

The results then obtained for the $\text{Ca}^{40}(d,p)\text{Ca}^{41}$ reaction at the six integral energies from 12 down to 7 MeV are displayed in Figs. 4 to 9. In each case the corresponding results obtained by Lee, Schiffer, Zeidman, Satchler, Drisko, and Bassel⁴ are shown for comparison; these results were derived from DWBA analysis using "best Z" deuteron parameters and proton optical parameters obtained from elastic-scattering data.

It can be seen that the two sets of angular distributions give comparable agreement with experiment from an over-all point of view. As far as the BHMM results are concerned, agreement at the lower deuteron energies is consistently not quite as good as at the higher deuteron energies. This may be correlated with the fact, as can be seen from Fig. 2, that agreement with the neutron elastic scattering is better at the higher of the two energies. In turn, the BHMM result receives its most significant contributions from a higher range of neutron energies the higher the deuteron energy. More extensive parameter fitting would be required to give better fits to the elastic-scattering data, and it would appear probable that the (d,p) angular distributions would thereby also be improved.

It is, however, highly satisfactory that the BHMM results compare as favorably as they do with experiment from such a simple approach to fitting the elastic-scattering data. The spectroscopic factors obtained are listed in Table II; once again the corresponding spectroscopic factors from DWBA analysis⁴ are shown for comparison. The BHMM values for S range from 0.49 to 0.60, giving an average value of 0.56 ± 0.04 . The DWBA values for S range from 0.74 to 0.96.

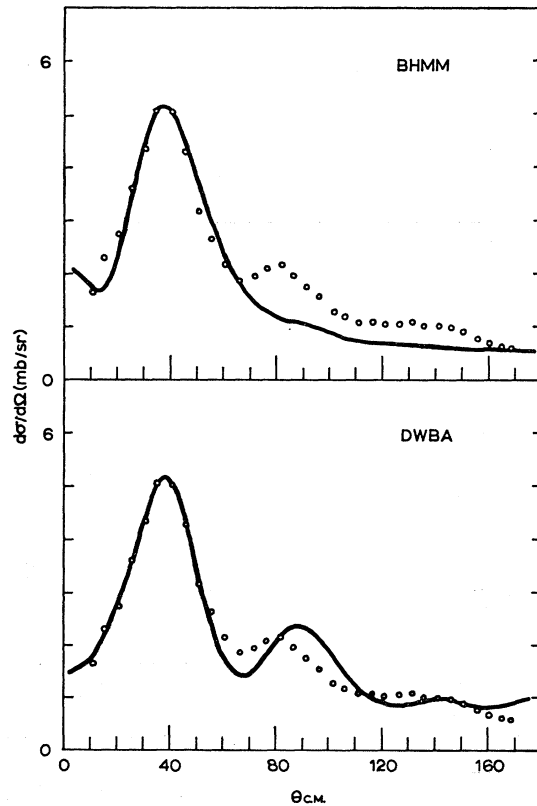


FIG. 7. Comparison of the predictions of BHMM and DWBA for the $\text{Ca}^{40}(d,p)\text{Ca}^{41}$ ground-state reaction at 9 MeV. The DWBA curve was generated with a "best-fit" type-Z deuteron potential (Ref. 4). The experimental points are also obtained from Ref. 4.

4. DISCUSSION

There is, at present, no conclusive way of deciding that the BHMM result presented here should be more reliable than the DWBA result, although we believe this to be the case.

It is true that, in view of the better agreement with experimental angular distributions at 12 MeV, a value of 0.60 may be more accurate than the average of 0.56. This is, however, still considerably lower than usual expectations which are often based on the following sum rule.

Suppose that Ψ_i is the full many-body wave function of the i th excited state of the final nucleus, so that Ψ_0 represents the wave function of the ground state. Let $\Lambda_c^N \Psi_0$ be the projection of the ground-state wave function on to the undisturbed core state, normalized to unity. Then clearly we can make the expansion

$$\Lambda_c^N \Psi_0 = \sum_i a_i \Psi_i, \quad (22)$$

where the spectroscopic factor S for the ground-state (d, p) reaction is $|a_0|^2$. At the same time, in view of the normalization of $\Lambda_c^N \Psi_0$, we have

$$\sum_i |a_i|^2 = 1. \quad (23)$$

If $S = |a_0|^2$ is significantly less than unity, the difference must therefore be made up from the sum of

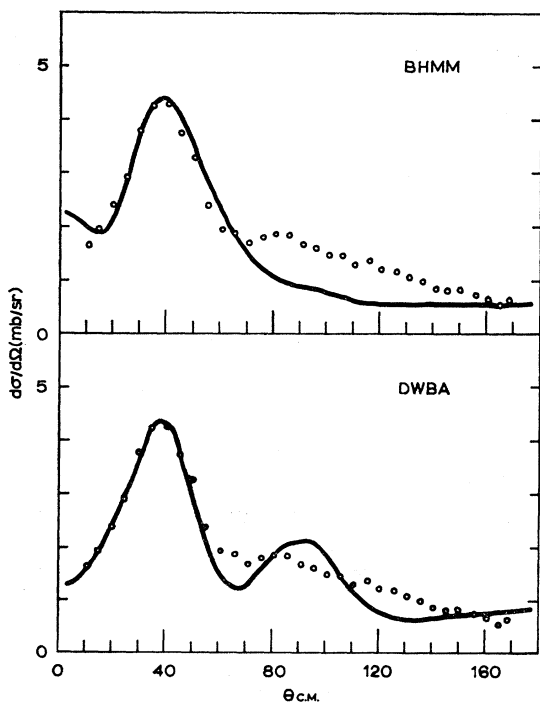


FIG. 8. Comparison of the predictions of BHMM and DWBA for the Ca⁴⁰(d, p)Ca⁴¹ ground-state reaction at 8 MeV. The DWBA curve was generated with a "best-fit" type-Z deuteron potential (Ref. 4). The experimental points are also obtained from Ref. 4.

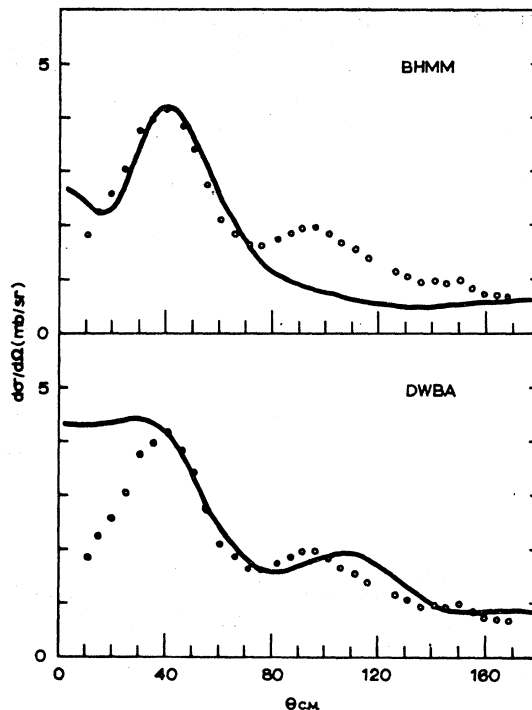


FIG. 9. Comparison of the predictions of BHMM and DWBA for the Ca⁴⁰(d, p)Ca⁴¹ ground-state reaction at 7 MeV. The DWBA curve was generated with a "best-fit" type-Z deuteron potential (Ref. 4). The experimental points are also obtained from Ref. 4.

squares of overlaps of the form $\langle \Lambda_c^N \Psi_0 | \Psi_i \rangle$ for $i \neq 0$. In cases where the final nucleus appears to exhibit a clearly identifiable single-particle spectrum up to excitations of, say, 8–10 MeV, it may be argued that such overlaps in this range should either be identically zero or at least very small. In such cases, it is argued that S should be very close to unity on the expectation that excited states Ψ_i above 8–10-MeV excitation can have little overlap with $\Lambda_c^N \Psi_0$.

We feel that this argument should not be taken too quantitatively. The density of excited states may increase very rapidly with increasing excitation and it appears to us possible that the sum of many small contributions from highly excited states may form significant contributions to Eq. (23). It appears to us undeniable that theories of nuclear structure are sufficiently speculative that absolute measurements of S are much more significant than theoretical estimates.

Naturally the sum-rule argument may be capable of indicating trends, and indeed an example of this seems to be the comparison between the Ca⁴⁸ and the Ca⁴⁰ reactions. The nucleus Ca⁴⁹ has a much cleaner single-particle spectrum than does Ca⁴¹ and the spectroscopic factor for the Ca⁴⁸(d, p)Ca⁴⁹ reaction might therefore be expected to be significantly closer to unity than that for the reaction Ca⁴⁰(d, p)Ca⁴¹. This is borne out by a (d, p) analysis. With averaged optical parameters, a BHMM analysis¹ gives a spectroscopic factor of 0.78

from the $\text{Ca}^{48}(d,p)\text{Ca}^{49}$ reaction, while the use of improved parameters along the lines of this paper can be shown to yield a value a little in excess of 0.8. Thus there seems no doubt that the spectroscopic factor relating to the $\text{Ca}^{48}\text{-Ca}^{49}$ overlap is indeed significantly greater than for the $\text{Ca}^{40}\text{-Ca}^{41}$ overlap.

Physically, a relatively low spectroscopic factor for some nuclei may perhaps be understood in terms of core deformation. It is well known that when a neutron is added even to a closed-shell nucleus, the centrifugal effects of its angular momentum produce a core deformation which, in fact, determines the quadrupole moment of the final nucleus and produces a smaller spectroscopic factor than might otherwise be expected.

Whether this is sufficient to understand a spectroscopic factor of 0.56 for the $\text{Ca}^{40}\text{-Ca}^{41}$ overlap depends on a quantitative estimate. Such an estimate may be attempted in terms of the collective-rotational model.⁹ This has been carried out on the Nilsson "strong-coupling" picture by Hodgson,¹⁰ who obtains the value $S=0.25$. While one cannot believe this number to be accurate, it does serve to indicate that a value of 0.56 is not necessarily too small.

Support for the contention that centrifugal deformation can significantly reduce a spectroscopic factor may be found in comparisons with $l=0$ reactions. An excellent comparison in this category can be made between the spectroscopic factors for the O^{16} ground-state (d,p) reaction, for which a d neutron is added, and for the (d,p) reaction to the first excited state of O^{17} which has an excitation of only 0.871 MeV and for which an s neutron is added; in the latter case, no centrifugal deformation can occur. At present we have only used an averaged set of optical parameters¹ to compare with experiment, but on this basis the above two spectroscopic factors are 0.53 and 0.85, respectively. While the use of more accurate parameters, along the lines of this paper may raise these figures slightly, the evidence for centrifugal deformation seems strong.

Similar analysis, using averaged parameters, shows that the ground-state (d,p) reaction on Mg^{24} with $l=2$ gives a spectroscopic factor in the vicinity of 0.5, while the neighboring Al^{27} and Si^{28} reactions, both of which have $l=0$, yield spectroscopic factors in the vicinity of 0.9.

Apart from the $\text{Ca}^{40}\text{-Ca}^{41}$ case discussed here we are accumulating spectroscopic factors from many (d,p) reactions by BHMM analysis and will present them in a later publication. Those referred to in the above discussion were mentioned in a preliminary way to strengthen the case that centrifugal distortion appears to play a significant role in decreasing spectroscopic factors. The main purpose of the present paper, how-

ever, has been to show that nucleon optical parameters chosen so as to yield reasonably close agreement with nucleon elastic-scattering data appear in the BHMM result, to yield (d,p) results in satisfactory agreement with experiment.

ACKNOWLEDGMENTS

We are grateful to R. J. W. Hodgson and Dr. B. H. J. McKellar and Dr. R. M. May for helpful discussions. This work was supported in part by the Science Foundation for Physics within the University of Sydney, and it is a pleasure to acknowledge the interest of its director, Professor H. Messel.

Note added in proof. An explanatory note may be made with regard to the recent paper by Bang and Pearson [Nucl. Phys. **A100**, 1 (1967)]. These authors write the direct component matrix element in the form

$$M_C = S^{1/2} \int_{\Sigma} d\mathbf{k}_p' \langle \psi_p^-(\mathbf{k}_p) | \psi_p^+(\mathbf{k}_p') \rangle \langle F_i^m(\mathbf{r}_n) | G(\mathbf{r}_n, \mathbf{k}_p') \rangle$$

but do not recognize an explicit form for the function G . Instead they generate a set of coupled integro-differential equations for the determination of this function. Since, however, the $\mathbf{k}_n' = \kappa$ term of our Eq. (5) is SM_C we have immediately

$$M_C = S^{1/2} \int_{\Sigma} d\mathbf{k}_p' \langle \psi_p^-(\mathbf{k}_p) | \psi_p^+(\mathbf{k}_p') \rangle \times \langle \psi_p^+(\mathbf{k}_p') F_i^m(\mathbf{r}_n) | V_{np} | \psi_d^+ \rangle.$$

By thus identifying the function G we see that evaluation of M_C by this method requires evaluation of the matrix element $\langle \psi_p^+(\mathbf{k}_p') F_i^m(\mathbf{r}_n) | V_{np} | \psi_d^+ \rangle$ for the same proton energy as in the (d,p) reaction in question, since $k_p' = k_p$. But this is the problem from which we started, since Eq. (4) itself is just this same matrix element except for the change to outgoing proton spherical waves. The crude approximations used by Bang and Pearson to obtain some estimate of $G(\mathbf{r}_n, \mathbf{k}_p')$ would appear far less reliable than use of ordinary DWBA techniques on Eq. (4) directly.

Our use of the above expression for M_C has not been for evaluation purposes, but to establish Eq. (7). Subsequent procedure is the evaluation of M_S which has the advantages referred to in the text.

It should also be recognized that criticisms of the sudden approximation made by Bang and Pearson are not relevant to the BHMM method. They refer to difficulties associated with substituting the sudden approximation directly into Eq. (4) and which have already been discussed in detail in Ref. 1.

APPENDIX

In order to transform \mathfrak{M}_S into a form convenient for substitution of the impulse approximation, we have removed the Λ_C operator from the right-hand side of

⁹ S. G. Nilsson, Kgl. Danske Videnskab. Selskab, Mat. Fys. Medd. **29**, 16 (1955). See also A. K. Kerman, *Nuclear Reactions* (North-Holland Publishing Company, Amsterdam, 1959), Vol. I, p. 427.

¹⁰ R. J. W. Hodgson (to be published).

the V_{np} matrix element in Eq. (6). We now formally show that this is justified.

To start with, the regime of direct nuclear reaction studies may be defined as follows: The full matrix element \mathfrak{M} for the (*d, p*) process [Eq. (1)] has two components, \mathfrak{M}_C and \mathfrak{M}_{CN} , where \mathfrak{M}_C is the direct component and \mathfrak{M}_{CN} may formally be written

$$\begin{aligned}\mathfrak{M}_{CN} &= \langle (1-\Lambda_C)\Psi^- | V_{np} | \Psi_d^+ \rangle \\ &= \langle \Psi^- | V_{np} | (1-\Lambda_C)\Psi_d^+ \rangle \\ &= \langle (1-\Lambda_C)\Psi^- | V_{np} | (1-\Lambda_C)\Psi_d^+ \rangle. \quad (\text{A1})\end{aligned}$$

The trivial identities

$$\begin{aligned}\langle \Lambda_C \Psi^- | V_{np} | (1-\Lambda_C)\Psi_d^+ \rangle \\ = \langle (1-\Lambda_C)\Psi^- | V_{np} | \Lambda_C \Psi_d^+ \rangle = 0\end{aligned} \quad (\text{A2})$$

are to be noted.

The basis of direct reaction studies is the expectation that, at least under appropriate circumstances, $\mathfrak{M}_{CN} \ll \mathfrak{M}_C$. It is then only the cross section generated by \mathfrak{M}_C which is calculated and compared with experiment.¹¹

Let us now write the matrix element \mathfrak{M}_S of Eq. (6) in the form

$$\begin{aligned}\mathfrak{M}_S &= \int_{\Sigma} d\mathbf{k}_p' \int_{\Sigma \neq \kappa} d\mathbf{k}_n' \langle \Lambda_C \Psi^-(\kappa, \mathbf{k}_p) | \Psi^+(\mathbf{k}_n', \mathbf{k}_p') \rangle \\ &\quad \times \langle \Psi^+(\mathbf{k}_n', \mathbf{k}_p') | V_{np} | \Psi^+ \rangle + m_S, \quad (\text{A3})\end{aligned}$$

where

$$\begin{aligned}m_S &= \int_{\Sigma} d\mathbf{k}_p' \int_{\Sigma \neq \kappa} d\mathbf{k}_n' \langle \Lambda_C \Psi^-(\kappa, \mathbf{k}_p) | \Psi^+(\mathbf{k}_n', \mathbf{k}_p') \rangle \\ &\quad \times \langle \Psi^+(\mathbf{k}_n', \mathbf{k}_p') | V_{np} | (\Lambda_C - 1)\Psi_d^+ \rangle. \quad (\text{A4})\end{aligned}$$

¹¹ It should be stressed that the direct process can predominate even when S is small, provided the initial deuteron energy is sufficiently high. It is true that the total probability for compound-nucleus formation is proportional to $(1-S)$. With sufficient energy available, however, compound-nucleus decay should occur primarily to high density states of high excitation.

From Eq. (A2), however, this may be rewritten as

$$\begin{aligned}m_S &= \int_{\Sigma} d\mathbf{k}_p' \langle \Lambda_C \Psi^-(\kappa, \mathbf{k}_p) | \Psi^+(\kappa, \mathbf{k}_p') \rangle \\ &\quad \times \langle \Psi^+(\kappa, \mathbf{k}_p') | V_{np} | (1-\Lambda_C)\Psi_d^+ \rangle. \quad (\text{A5})\end{aligned}$$

We also have immediately¹

$$\begin{aligned}\langle \Lambda_C \Psi^-(\kappa, \mathbf{k}_p) | \Psi^+(\kappa, \mathbf{k}_p') \rangle \\ = S \langle \psi_p^-(\mathbf{k}_p, \mathbf{r}_p) | \psi_p^+(\mathbf{k}_p', \mathbf{r}_p) \rangle \\ = S \left\{ \delta(\mathbf{k}_p - \mathbf{k}_p') + \frac{i}{\pi} \delta(k_p^2 - k_p'^2) f(\mathbf{k}_p, \mathbf{k}_p') \right\}, \quad (\text{A6})\end{aligned}$$

where f is the usual proton elastic scattering amplitude so normalized that $|f|^2$ is directly the differential cross section. Hence

$$\begin{aligned}m_S &= S \langle \Psi^+(\kappa, \mathbf{k}_p) | V_{np} | (1-\Lambda_C)\Psi_d^+ \rangle \\ &\quad + \frac{iSk_p}{2\pi} \int d\Omega f(\theta) \langle \Psi^+(\kappa, \mathbf{k}_p') | V_{np} | (1-\Lambda_C)\Psi_d^+ \rangle, \quad (\text{A7})\end{aligned}$$

where θ is the angle between \mathbf{k}_p' and \mathbf{k}_p , and $d\Omega$ is the element of solid angle of \mathbf{k}_p' , and $k_p' = k_p$.

The first term of m_S is precisely S multiplying a matrix element which is the compound nucleus component \mathfrak{M}_{CN} (apart from the change to outgoing spherical waves in Ψ^+). The second term has this same compound nucleus component convoluted over proton scattering angles in the manner analyzed in BHMM for the direct component of the matrix element.

Thus m_S is manifestly a compound nucleus component. Within the direct-reaction regime, therefore, the matrix element \mathfrak{M}_S may be defined by either Eq. (6) or Eq. (A3) without m_S .